A novel {Fe^{I}–Fe^{II}–Fe^{II}–Fe^{I}} iron thiolate carbonyl assembly which electrocatalyses hydrogen evolution†

Cédric Tard, Xiaoming Liu, David L. Hughes and Christopher J. Pickett*

Received (in Cambridge, UK) 29th July 2004, Accepted 24th September 2004
First published as an Advance Article on the web 11th November 2004
DOI: 10.1039/b411559g

A novel tetra-iron thiolate carbonyl assembly is described in which two dithiolate tetracarbonyl di-iron centres with a 'butterfly' configuration of the {2Fe3S}-cores are fused by two bridging thiolates which form a central planar 2Fe2S unit and comprise the first example of a chain of four metal–metal bonded iron atoms supported by a bridging sulfur framework; the assembly electrocatalyses hydrogen evolution.

A dithiolate di-iron unit co-ligated by CO and CN and attached *via* a bridging cysteinyl ligand to a 4Fe4S cluster forms the active site of all-iron hydrogenase, the H-cluster. Since this structure was uncovered,[1,2] there has been much activity in the synthesis of 2Fe2S and 2Fe3S assemblies which model key features of the sub-site.[3] There have also been several studies of the electrocatalytic activity of such di-iron assemblies. However, all involve reduction of an Fe^{I}–Fe^{I} centre to the Fe^{0}–Fe^{I} level and/or reduction of protonated Fe^{I}–Fe^{I} assemblies with phosphine or other abiological co-ligands; none possesses a {2Fe3S} core and all function at potentials considerably negative of that for reversible hydrogen evolution/uptake.[4–7]

In its resting state, the di-iron sub-site is most probably an Fe^{I}–Fe^{II} arrangement with the paramagnetic Fe^{I} centre distal to the cluster[8] and various DFT studies invoke turnover at the Fe^{I}–Fe^{I} level.[9–14] Herein we describe the synthesis and structure of a novel metal–metal bonded four-iron system which can be viewed as comprising two {2Fe3S} units fused by the bridging of two thiolates to give a unique (Fe^{I}–Fe^{II}–Fe^{II}–Fe^{I}) assembly. We show that this system undergoes two successive reversible single electron-transfer steps and is capable of electrocatalysing proton reduction at the all-Fe^{I} level.

Dithiolate thioether ligands of the type $MeC(CH_2SR)(CH_2S)_2$ (R = various groups), derived from $MeC(CH_2SH)_3$ **A**, afford {2Fe3S} complexes of the type $[Fe_2\{MeC(CH_2SR)(CH_2S)_2\}(CO)_5]$ **B** in moderate yield upon refluxing with $Fe_3(CO)_{12}$ in toluene.[15,16] Under the same conditions, the parent trithiol **A** was found to produce largely intractable insoluble material together with a soluble fraction from which we have now isolated by chromatography **C**, $[Fe_4\{MeC(CH_2S)_3\}_2(CO)_8]$, as deep-red crystalline needles [ν(CO), CH_2Cl_2: 2046 cm^{-1} (s), 1988 cm^{-1} (broad, s), 1947 cm^{-1} (sh, m)] in *ca.* 8% yield. It is quite possible that **C** is formed by dimerisation of **B** (R = H) by oxidative elimination of dihydrogen and loss of CO but we have not studied this.

† Electronic supplementary information (ESI) available: experimental and simulated cyclic voltammograms of 1.5 mM of **C** in the presence of 33 mM $LutH^{+}$ at 100 mV s^{-1}. See http://www.rsc.org/suppdata/cc/b4/b411559g/

Crystal structure analysis‡ of **C** shows two independent, but essentially identical, molecules in the crystal. One of these molecules, with selected dimensions, is shown in Fig. 1. Each molecule is arranged about a centre of symmetry and thus has a central *planar* thiolate-bridged di-iron unit, that is the rhomb formed by Fe(2), S(3), Fe(2′), and S(3′). These inner iron atoms Fe(2) and Fe(2′) are linked to Fe(1) and Fe(1′) respectively by two bridging thiolates in the butterfly configuration characteristic of dinuclear {2Fe2S}- and {2Fe3S}-carbonyls such as $[Fe_2\{MeC(CH_2SMe)(CH_2S)_2\}(CO)_5]$.[15,16] The short Fe(1)···Fe(2) distances, with mean value 2.543(5) Å, suggest a degree of metal–metal bonding. As far as we are aware, **C** represents the first example of a molecular chain of four metal–metal bonded iron atoms supported by a bridging sulfur framework.[17]

The formal oxidation states of the two *exo*-iron atoms Fe(1) and Fe(1′) can be considered as Fe^{I} and those of the two internal iron atoms Fe(2) and Fe(2′) as Fe^{II}. Thus in the Fe^{I}–Fe^{II}–Fe^{II}–Fe^{I} metal–metal bonding completes an 18-electron configuration about each metal atom in an electron-precise 66e structure. Fig. 2 shows the cyclic voltammetry of **C** {vitreous carbon; CH_2Cl_2—0.5 M $[NBu_4][BF_4]$; 100 mVs^{-1}; RT}. Two successive diffusion-controlled one-electron reductions are observed with $E^{o\prime}$ at −0.70 and −1.07 V *versus* {Ag/AgCl, CH_2Cl_2, 0.45 M

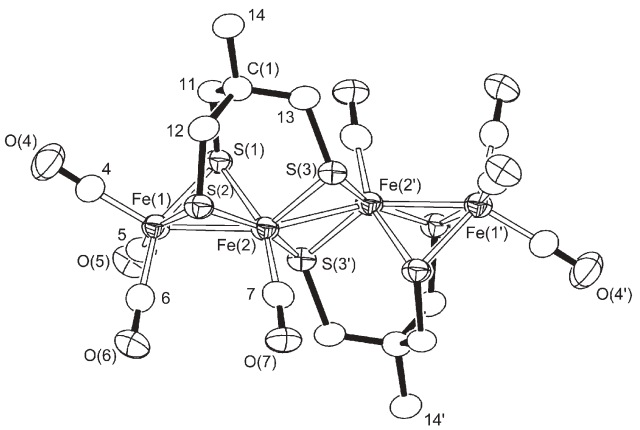

Fig. 1 One of the two independent molecules of **C**. Hydrogen atoms have been omitted for clarity. Thermal ellipsoids are drawn at the 50% probability level. Selected molecular dimensions (mean values of the two molecules, with sds in parentheses): Fe(1)–Fe(2) 2.543(5), Fe(1)–S(1) 2.264(3), Fe(1)–S(2) 2.252(3), Fe(1)–C(4) 1.789(17), Fe(1)–C(5) 1.780(14), Fe(1)–C(6) 1.803(7), Fe(2)–Fe(2′) 2.651(9), Fe(2)–S(1) 2.288(2), Fe(2)–S(2) 2.251(5), Fe(2)–S(3) 2.238(3), Fe(2)–S(3′) 2.233(9), Fe(2)–C(7) 1.771(3)Å, Fe(1)–Fe(2)–Fe(2′) 147.0(2), Fe(1)–S(1)–Fe(2) 67.93(12), Fe(1)–S(2)–Fe(2) 68.77(9), Fe(2)–S(3)–Fe(2′) 72.7(2)°.

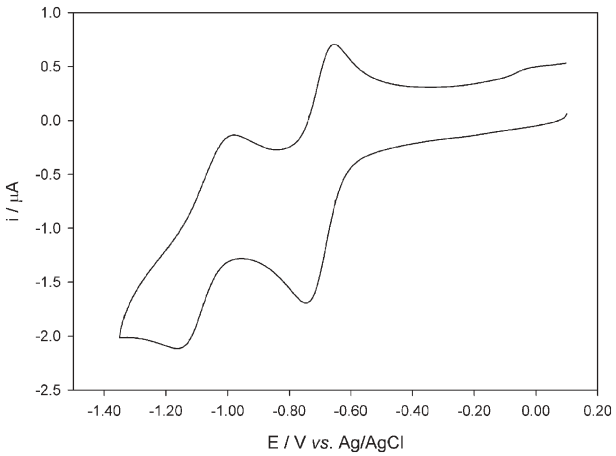

Fig. 2 Cyclic voltammogram of **C** at 100 mV s^{-1} showing successive reversible and quasi-reversible single-electron transfer steps. A further irreversible one-electron reduction is observed near −2 V.

$[NBu_4][BF_4]$, 0.05 M $[NBu_4]Cl$} respectively. Thus there is a linear dependence of peak currents on [scan-rate]$^{1/2}$, the ratios of the forward and back peak currents for each process are close to unity, and the peak potential separation ΔE for the primary process of 75 mV at 100 mVs^{-1} is close to that observed for the reversible oxidation of ferrocene under the same experimental conditions. The secondary reversible step shows a large ΔE of 175 mV corresponding to slow electron-transfer kinetics, *i.e.* quasi-reversibility, and is indicative of structural or spin-state re-organisation accompanying the electron-transfer step.

The difference in the values $E^{\circ\prime}$ for the primary and secondary reduction steps of *ca.* 310 mV shows moderately strong electronic communication in the system.[18] Thus addition of the first and second electrons do not take place to electronically insulated localised redox orbitals. It seems most likely that addition of the first electron populates a metal–metal anti-bonding orbital on the central di-iron pair, with the addition of the second electron to this SOMO resulting in concerted cleavage of the central metal–metal

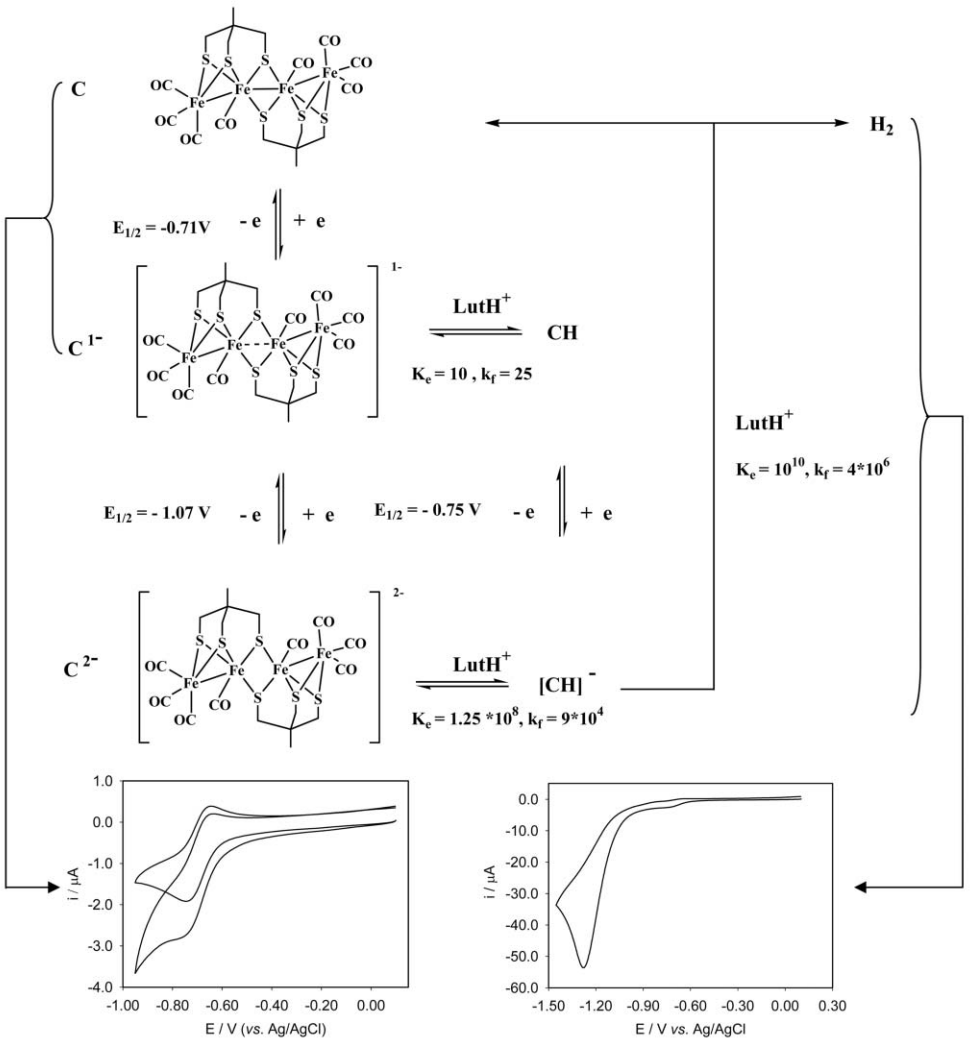

Scheme 1 Mechanism for hydrogen evolution electrocatalysed by **C**. The equilibrium constants K_e (dimensionless) and the forward rate constants k_f ($M^{-1}L\ s^{-1}$) were those used to simulate the voltammogram in Fig. 4, ESI.† The left inset shows the experimental cyclic voltammetric response of the $\mathbf{C}/\mathbf{C}^{1-}$ couple (1.5 mM, 100 mV s^{-1}) before and after addition of LuH^+ (33 mM); the right inset shows the overall response in the presence of the acid.

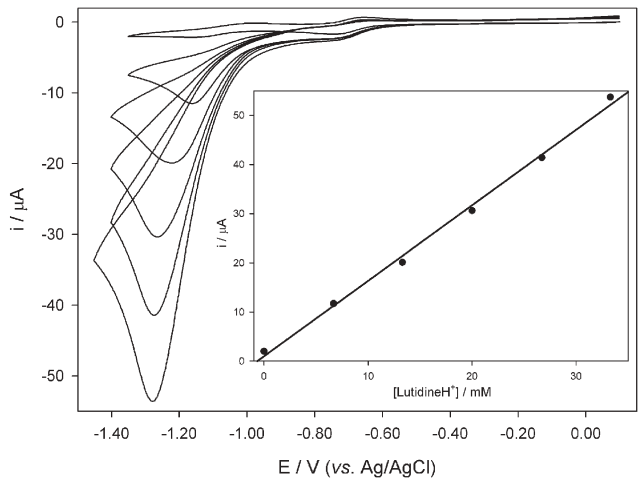

Fig. 3 The cyclic voltammetric response of **C** in the presence of LuH^+. The inset shows the linear plot of peak currents corresponding to those in the voltammograms against the concentration of the acid.

bond, a structural re-organisation consistent with the quasi-reversibility of this second electronation, Scheme 1. Cleavage of the central metal–metal bond would conserve the 18-electron configuration about each of the iron atoms in the Fe^I–Fe^I–Fe^I–Fe^I assembly. Fig. 3 shows the cyclic voltammetric responses of **C** in the presence of 2,6-dimethylpyridinium ($LutH^+$) tetrafluoroborate as a source of protons (pK_a = 14.05, MeCN)[19] in the CH_2Cl_2—0.5 M $[NBu_4][BF_4]$ electrolyte and the linear dependence of the catalytic peak current on the concentration of $LutH^+$. It is evident that electrocatalytic proton reduction is mediated by accessing the di-anionic all-Fe^I level. Bulk electrolysis experiments were performed at −1.5 V *versus* Ag/AgCl, and gas chromatographic sampling after the passage of 9 F (mole **C**)$^{-1}$ confirmed the formation of dihydrogen in 85 ± 5% current yield.

The first single electron-transfer step of **C** becomes partially reversible in the presence of the acid source and the current is enhanced towards a two-electron process, Fig. 3 and Scheme 1. This is accommodated by the electrocatalytic mechanism shown in Scheme 1 which provides the basis for digital simulation of the cyclic voltammetric behaviour in the presence of $LutH^+$ (see Fig. 4, ESI†). Direct reduction of $LutH^+$, which occurs on vitreous carbon with a peak potential 60 mV negative of that for the electrocatalytic reduction, is suppressed in the presence of **C** as protons are removed rapidly from $LutH^+$ by the turnover of **C** in the diffusion layer.

As noted above, several di-iron carbonyl thiolate systems have been shown to electrocatalyse proton reduction but these generally involve reduction of an Fe^I–Fe^I system to the Fe^I–Fe^0 or Fe^0–Fe^0 levels,[4–7] whereas it is likely that the di-iron sub-site of the enzyme system protonates and reduces at the Fe^I–Fe^I level. Exceptions to this have hitherto been confined to mixed cyanide–tertiary phosphine anion assemblies where enhanced basicity allows protonation at cyanide and/or the metal–metal bond.[7] So far, all synthetic electrocatalytic assemblies are energetically rather than kinetically inefficient in that they function at overpotentials far removed from the potential of the H^+/H_2 system on Pt under the same conditions. For example $LutH^+$ reduction on bright platinum occurs at E_p = −0.67 V *versus* Ag/AgCl and the synthetic challenge remains to design sub-site systems which function efficiently at low overpotentials.

We thank the BBSRC and the John Innes Foundation for supporting this work.

Cédric Tard, Xiaoming Liu, David L. Hughes and Christopher J. Pickett*
Department of Biological Chemistry, John Innes Centre, Norwich, UK NR4 7UH

Notes and references

‡ *Crystal data for* $[(Fe_2(CO)_4\{MeC(CH_2S)_3\})_2]$: $C_{18}H_{18}Fe_4O_8S_6$, M = 778.1. Triclinic, space group $P\bar{1}$ (no. 2), a = 9.837(2), b = 12.119(2), c = 14.101(3) Å, α = 101.85(3), β = 105.13(3), γ = 114.56(3)°, V = 1378.5(5) Å^3, Z = 2, D_c = 1.875 g cm^{-3}, $F(000)$ = 780, T = 140(1) K, μ(Mo–Kα) = 25.6 cm^{-1}, λ(Mo–Kα) = 0.71069 Å. Deep red, wafer-thin needles. Rigaku R-Axis IIc image-plate diffractometer; θ_{max} = 25.4°, 7931 reflections total, 4696 unique (Rint = 0.098), 3056 with $I > 2\sigma(I)$. Structure by direct methods; refinement, on F^2's, to wR_2 = 0.135 and R_1 = 0.085 for all 4696 reflections weighted $w = [\sigma^2(F_o^2) + (0.0563\ P)^2]^{-1}$ with $P = (F_o^2 + 2F_c^2)/3$; for the 'observed' data only, R_1 = 0.054. Highest peaks (to *ca.* 0.51 *e* Å^{-3}) in final difference map close to the iron atoms. CCDC 246858. See http://www.rsc.org/suppdata/cc/b4/b411559g/ for crystallographic data in .cif or other electronic format.

1 J. W. Peters, W. N. Lanzilotta, B. J. Lemon and L. C. Seefeldt, *Science*, 1998, **282**, 1853.
2 Y. Nicolet, C. Piras, P. Legrand, C. E. Hatchikian and J. C. Fontecilla-Camps, *Folding Des.*, 1999, **7**, 13.
3 D. J. Evans and C. J. Pickett, *Chem. Soc. Rev.*, 2003, **32**, 268.
4 S. Ott, M. Kritikos, B. Akermark, L. C. Sun and R. Lomoth, *Angew. Chem., Int. Ed.*, 2004, **43**, 1006.
5 J. F. Capon, F. Gloaguen, P. Schollhammer and J. Talarmin, *J. Electroanal. Chem.*, 2004, **566**, 241.
6 D. S. Chong, I. P. Georgakaki, R. Mejia-Rodriguez, J. Samabria-Chinchilla, M. P. Soriaga and M. Y. Darensbourg, *Dalton Trans.*, 2003, 4158.
7 F. Gloaguen, J. D. Lawrence, M. Schmidt, S. R. Wilson and T. B. Rauchfuss, *J. Am. Chem. Soc.*, 2001, **123**, 12518.
8 A. L. De Lacey, C. Stadler, C. Cavazza, E. C. Hatchikian and V. M. Fernandez, *J. Am. Chem. Soc.*, 2000, **122**, 11232.
9 Z. X. Cao and M. B. Hall, *J. Am. Chem. Soc.*, 2001, **123**, 3734.
10 M. Bruschi, P. Fantucci and L. De Gioia, *Inorg. Chem.*, 2002, **41**, 1421.
11 Z. P. Liu and P. Hu, *J. Am. Chem. Soc.*, 2002, **124**, 5175.
12 M. Bruschi, P. Fantucci and L. De Gioia, *Inorg. Chem.*, 2003, **42**, 4773.
13 M. Bruschi, P. Fantucci and L. De Gioia, *Inorg. Chem.*, 2004, **43**, 3733.
14 H. J. Fan and M. B. Hall, *J. Am. Chem. Soc.*, 2001, **123**, 3828.
15 M. Razavet, S. C. Davies, D. L. Hughes and C. J. Pickett, *Chem. Commun.*, 2001, 847.
16 M. Razavet, S. C. Davies, D. L. Hughes, J. E. Barclay, D. J. Evans, S. A. Fairhurst, X. M. Liu and C. J. Pickett, *Dalton Trans.*, 2003, 586.
17 W. Imhof, *Organometallics*, 1999, **18**, 4845.
18 D. E. Richardson and H. Taube, *Coord. Chem. Rev.*, 1984, 107.
19 K. Isutzu, *Acid–Base Dissociation Constants in Dipolar Aprotic Solvents: IUPAC Chemical Data Series No. 35*, Blackwell Scientific Publications, Boston, 1990.